Journal of Electroanalytical Chemistry 716 (2014) 49–52

Contents lists available at ScienceDirect

Journal of Electroanalytical Chemistry

journal homepage: www.elsevier.com/locate/jelechem

Electrochemical quartz crystal microbalance study on the oxygen reduction reaction in Li^+ containing DMSO solution

Xiao Jie [a], Kohei Uosaki [a,b,*]

[a] Global Research Center for Environment and Energy based on Nanomaterials Science (GREEN), National Institute for Materials Science (NIMS), Tsukuba 305-0044, Japan
[b] International Center for Materials Nanoarchitectonics (WPI-MANA), NIMS, Tsukuba 305-0044, Japan

ARTICLE INFO

Article history:
Available online 18 October 2013

Keywords:
Lithium air battery
Oxygen reduction reaction
Electrochemical quartz crystal microbalance
Lithium superoxide
DMSO

ABSTRACT

Electrochemical quartz crystal microbalance (EQCM), which can detect surface mass change in ng scale, was employed to investigate the deposition of $Li–O_2$ species on a gold electrode upon reduction of oxygen in a DMSO solution containing Li^+ cation. In relatively positive potential region, the mass per mol-electron (mpe) calculated from the slope of the relation between mass change and accumulated charge was 37 g/mol-e, indicating the deposition of lithium superoxide (LiO_2) with the reaction of $O_2 + e^- + Li^+ \rightarrow LiO_2$. As the potential became more negative, where superoxide ($O_2^{\cdot-}$) was formed in Li^+ free solution, the mpe became much smaller (ca. 7 g/mol-e), suggesting the formation of $O_2^{\cdot-}$, some of which were diffused away.

1. Introduction

Although Li-air battery attracts much research interest because of high theoretical energy density and power density [1–3], the performance of Li-air battery is still very low because of the slow kinetics and low reversibility of electrodeposition of $Li–O_2$ species, i.e., oxygen reduction reaction in non-aqueous solutions with Li^+ cation, which is the discharge process of Li-air battery [4,5]. Thus, the understanding of oxygen reduction reaction mechanism in non-aqueous solution containing Li^+ is one of the keys [6–8] to realize Li-air battery but the investigation of ORR in non-aqueous solution particularly with Li^+ cation is still limited.

Although there is no doubt that lithium peroxide (Li_2O_2) is the main product after the cell discharge without other side reactions [9,10], lithium superoxide (LiO_2) was detected as an intermediate product by in-situ surface enhanced Raman spectroscopy (SERS) during discharge process [11,12]. Peng et al. suggested that ORR proceeds by electrochemical/chemical (EC) mechanism as oxygen is first reduced to superoxide $O_2^{\cdot-}$ followed by a chemical reaction to form LiO_2, and then disproportionate to Li_2O_2 [12]. On the other hand, Hassoun et al. proposed that ORR proceeds via one-step reduction of oxygen with Li^+ cation to generate LiO_2 followed by further reduction to Li_2O_2 and lithium oxide (Li_2O) [13].

Electrochemical quartz crystal microbalance (EQCM) is a very powerful technique to understand electrochemical reaction on electrode surface as it can detect the adsorption/deposition in ng scale [14].

Here we have employed EQCM to investigate the lithium–oxygen reactions in DMSO solution at a gold electrode in potential region relevant to ORR reaction in Li-air battery operation. Potential dependent deposition mechanisms of $Li–O_2$ species were distinguished according to the potential. In relatively positive potential region, the mass per mol-electron (mpe) calculated from the slope of the relation between mass change and accumulated charge was 37 g/mol-e, indicating the deposition of lithium superoxide (LiO_2) with the reaction of $O_2 + e^- + Li^+ \rightarrow LiO_2$. As the potential became more negative, where superoxide ($O_2^{\cdot-}$) was formed in Li^+ free solution, the mpe became much smaller (ca. 7 g/mol-e), suggesting the formation of $O_2^{\cdot-}$, some of which were diffused away.

2. Experimental

All chemicals, tetrabutylammonium hexafluorophosphate ($TBAPF_6$), lithium hexafluorophosphate ($LiPF_6$), and anhydrous dimethyl sulfoxide (DMSO), were of electrochemical grade (Sigma–Aldrich) and used without further purification.

A three compartment, three-electrode cell with a Ag/Ag^+ reference electrode (RE) and a platinum wire counter electrode (CE) was used for electrochemical measurements. A Au thin film ($\phi = 3$ mm) deposited on a 10 MHz AT-cut quartz crystal (Hokuto Denko) was used as a working electrode (WE) for the electrochemical and EQCM measurements. The Ag/Ag^+ reference electrode, which was a silver wire immersed in a DMSO solution containing 0.1 M $TBAPF_6$ and 0.01 M $AgNO_3$, was placed in the RE compartment separated from the working electrode (WE) compartment

---

[*] Corresponding author at: Global Research Center for Environment and Energy based on Nanomaterials Science (GREEN), National Institute for Materials Science (NIMS), Tsukuba 305-0044, Japan. Tel.: +81 29 895 3213.
E-mail address: uosaki.kohei@nims.go.jp (K. Uosaki).

1572-6657/$ - see front matter
http://dx.doi.org/10.1016/j.jelechem.2013.10.010

by a Luggin capillary, the tip of which was positioned very close to the WE to reduce the uncompensated IR drop. All the potentials in this paper are presented with respect to Li/Li$^+$, which is -3.58 V vs. the Ag/Ag$^+$ reference electrode. The CE compartment was isolated from the WE by a glass frit.

All electrochemical experiments were carried out in a glove box where water concentration was kept below 1 ppm using a computer controlled electrochemical measurement system (Hokuto Denko, HZ5000). In order to investigate the deposition of Li–O_2 species at the same surface state, only the first electrochemical measurements at the fresh gold electrode were used for discussions.

The resonant frequency of the quartz crystal electrode was recorded simultaneously with the electrode potential and current by a data logger (GRAPH-TEC, GL-200A) interfaced to a high-resolution frequency counter (Hokuto Denko, HQ-101D) with a sampling time of 0.2 s. The mass change (Δm) was estimated from the resonant frequency change (Δf) according to the Sauerbrey equation [15,16]:

$$\Delta m = -C_f \Delta f \tag{1}$$

where C_f is the sensitivity factor of the 10 M Hz AT-cut quartz crystal as calibrated to be 5.4 ng Hz^{-1} cm^{-2} by Ag deposition in DMSO and aqueous solutions [17,18].

All of the measurements were carried out after the solution was saturated by purging purified oxygen or Argon gas through the solution for at least 30 min.

3. Results and discussion

Fig. 1 shows simultaneously recorded (a) current and (b) frequency change as a function of potential of the gold electrode obtained in oxygen saturated DMSO solution containing 0.1 M TBAPF$_6$ (···) and 0.1 M LiPF$_6$ (□□□) as well as in Ar saturated DMSO solution containing 0.1 M TBAPF$_6$ or 0.1 M LiPF$_6$ (---) when the potential was scanned by 20 mV/s. While no obvious current was observed in the Ar saturated solutions, a symmetric redox wave with peak separation of 320 mV corresponding to $O_2/O_2^{\cdot -}$ redox couple was observed in the oxygen saturated Li$^+$ free solution, indicating that O_2 reduction reaction at gold electrode in DMSO solution containing large cation such as TBA$^+$ is quasi-reversible as reported in 1960s [19]. No obvious mass change during the $O_2/O_2^{\cdot -}$ redox process was detected (Fig. 1b), confirming that $O_2/O_2^{\cdot -}$ redox reaction in TBAPF$_6$ takes place not on the surface but in the solution bulk [20,21].

Totally different behavior was observed in the DMSO solution containing 0.1 M LiPF$_6$. Cathodic current started to flow at more positive potential than in TBA$^+$ solution, a small and large cathodic peak were observed at ca. 2.65 and 2.36 V, respectively, but only very small anodic peak was observed. Actually the current sharply decreased to almost 0 after the second cathodic peak at 2.36 V, implying the generation of some insulating layer on the electrode surface.

Fig. 1b shows large mass increase during the potential cycle. The mass started to increase as soon as cathodic current started to flow. During the first potential cycle, total 373 Hz decrease in the frequency, i.e., 2016 ng/cm^2 increase in the mass, was detected. Fig. 1c shows the mass change as a function of the integrated cathodic charge obtained by using the results of Fig. 1a and b. We can divide the potential region into four regions based on the potential dependence of the mass change with respect to the cathodic charge as shown in Fig. 1.

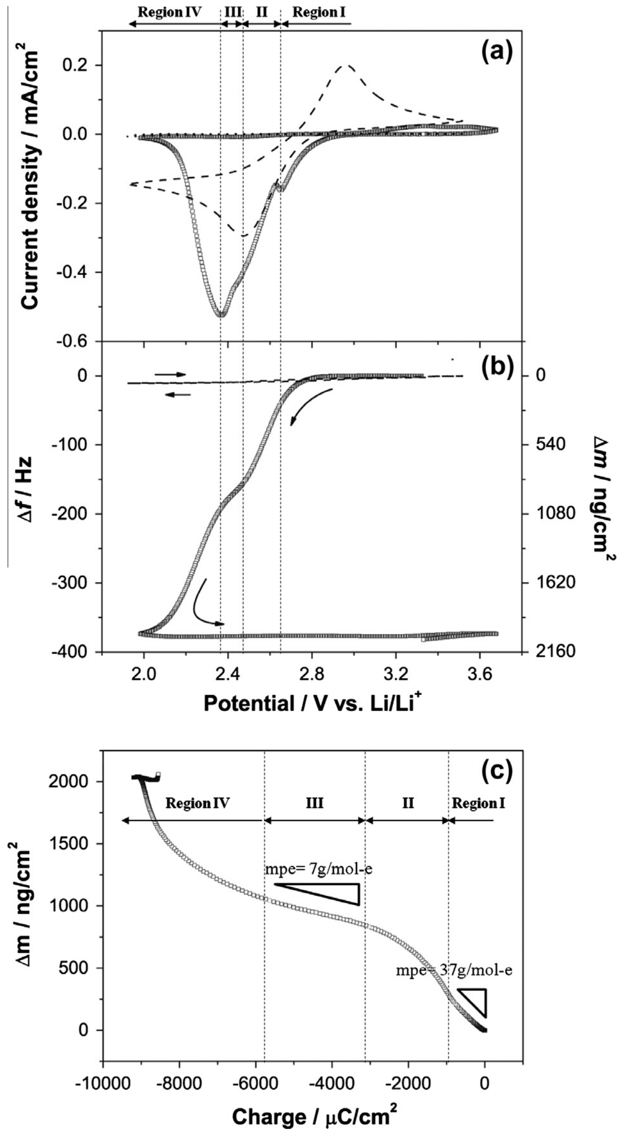

Fig. 1. Simultaneously obtained (a) current and (b) frequency change and corresponding mass change at the gold electrode as a function of potential in DMSO solutions when potential was swept by 20 mV/s. (c) Mass change as a function of integrated charge based on the results of (a) and (b). (---): Oxygen saturated 100 mM TBAPF$_6$/DMSO solution, (···): Ar saturated 100 mM LiPF$_6$/DMSO solution, and (□□□): oxygen saturated 100 mM LiPF$_6$/DMSO solution.

Initially the mass increased almost linearly with the charge up to ca. 2.65 V, which agrees with the first peak potential. In this region (Region I), the mass per mol-electron (mpe), which was calculated from the slope of the relation between mass change and accumulated charge, was ca. 37 g/mol-e, suggesting the deposition of LiO_2, the molecular weight of which is 39 g. This result and the positive shift of cathodic current flow as well as the fact that the peak height of the first peak at 2.65 V was linearly related with the concentration of Li$^+$ (data not shown) suggest that the first step of ORR in Li$^+$-containing electrolyte is not superoxide formation by:

$$O_2 + e^- \rightarrow O_2^{\cdot -} \tag{2}$$

but by:

$$O_2 + e^- + Li^+ \rightarrow LiO_2 \tag{3}$$

It has been reported that the onset potential for O_2 reduction reaction becomes more positive in the presence of protons or metal cations such as Fe, Zn, Mn, and Co [22]. The apparent stabilization of superoxide by these cations and adsorption of the product are accounted for the anodic shift of the reduction potential.